Final Technical Report for AFOSR Award Number: F49620-97-1-0177

SiGeC Optoelectronic Devices

Report Time Period: 15 January 1995 through 14 January, 1998

Professor James Kolodzey
Department of Electrical and Computer Engineering
University of Delaware
216 Evans Hall
Newark, DE 19716
USA

tel: (302)-831-1164
fax: (302)-831-4316
email: kolodzey@ee.udel.edu
web: http://www.ee.udel.edu/~kolodzey

Contents

20000526 013

DTIC QUALITY INSPECTED 3

REPORT DOCUMENTATION PAGE

AFRL-SR-BL-TR-00-

0174

Public reporting burden for this collection of information is estimated to average 1 hour per response, including the time for reviewing ins reviewing the collection of information. Send comments regarding this burden estimate or any other aspect of this collection of informati Information Operations and Reports, 1215 Jefferson Davis Highway, Suite 1204, Arlington, VA 22202-4302, and to the Office of Managem completing and Directorate for

1. AGENCY USE ONLY *(Leave blank)*	2. REPORT DATE	3. RE... ...TYPE AND DATES COVERED
		Final 01 May 97 to 31 Oct 97

4. TITLE AND SUBTITLE
SIGEC Electroluminescent Devices

5. FUNDING NUMBERS
61102F
2305/FS

6. AUTHOR(S)
Professor Kolodzey

7. PERFORMING ORGANIZATION NAME(S) AND ADDRESS(ES)
University of Delaware
210 Hullihen Hall
Newark DE 19716-1551

8. PERFORMING ORGANIZATION REPORT NUMBER

9. SPONSORING/MONITORING AGENCY NAME(S) AND ADDRESS(ES)
AFOSR/NE
801 N Randolph Street Rm 732
Arlington, VA 22203-1977

10. SPONSORING/MONITORING AGENCY REPORT NUMBER
F49620-97-1-0177

11. SUPPLEMENTARY NOTES

12a. DISTRIBUTION AVAILABILITY STATEMENT
APPROVAL FOR PUBLIC RELEASE, DISTRIBUTION UNLIMITED

12b. DISTRIBUTION CODE

13. ABSTRACT *(Maximum 200 words)*

These result in a better I-V characteristic with smaller leakage current and higher breakdown voltage. Our electrical study indicated that by careful control the growth conditions and carbon percentages, high-quality devices could be fabricated. These results indicate that strain, composition, and substrate orientation all play roles in quantum dot formation and provide different vehicles to control the self-assembly and self-organization of quantum dots for device applications.

14. SUBJECT TERMS			15. NUMBER OF PAGES
			16. PRICE CODE
17. SECURITY CLASSIFICATION OF REPORT	18. SECURITY CLASSIFICATION OF THIS PAGE	19. SECURITY CLASSIFICATION OF ABSTRACT	20. LIMITATION OF ABSTRACT
UNCLASSIFIED	UNCLASSIFIED	UNCLASSIFIED	UL

Standard Form 298 (Rev. 2-89) (EG)
Prescribed by ANSI Std. 239.18
Designed using Perform Pro, WHS/DIOR, Oct 94

1. Electrical Properties of $Si_{1-x-y}Ge_xC_y$ and $Ge_{1-y}C_y$ Alloys

The structural and electrical properties of $Si_{1-x-y}Ge_xC_y$ and $Ge_{1-y}C_y$ alloys have been examined by Hall effect measurements, dc electrical measurements, and X-ray diffraction. Carbon incorporation in the molecular beam epitaxy grown SiGe and Ge layers has great influence on the carrier mobility and the I-V characteristics.

Hall effect measurements showed that the addition of carbon could increase the hole mobility in GeC as compared to that in pure Ge. One possible reason is that the addition of carbon can improve the crystal quality, which strongly affects the carrier mobility. I-V characteristics of SiGeC/Si and GeC/Si heterojunction diodes under reverse bias showed that leakage current decreased with increasing carbon, and the breakdown voltage increased with increasing carbon. Forward I-V characteristics showed that the turn-on voltage increased with increasing carbon.

Introduction

Recently, the growth and characterization of the Group IV elements (C, Si, Ge) have been attracting more attention for use in heterojunction (HJ) devices compatible with Si technology. Although the equilibrium solubility of C in Si and Ge is very low, $Si_{1-x-y}Ge_xC_y$ and $Ge_{1-y}C_y$ alloys can be synthesized by non-equilibrium growth method such as molecular beam epitaxy (MBE) at relatively low growth temperature. The additional C in SiGe and Ge affects the strain compensation, interface roughness, carrier transport, bandgap energy and the energy band offsets. Although the structure and optical properties of $Si_{1-x-y}Ge_xC_y$ and $Ge_{1-y}C_y$ alloys have been reported, the electrical properties are not yet well understood.

This report focuses on the electrical properties of p-type Ge-rich SiGeC and GeC alloys grown on n-type Si-substrate by MBE. Hall effect measurements have been used to study the effects of carbon on the charge transport. I-V characteristics of SiGeC/Si and GeC/Si HJ diodes under reverse bias have

been investigated to show the influence of carbon on the reverse leakage current and breakdown voltage.

Experiments

The SiGeC and GeC epilayer were grown by MBE in an EPI620 system. The Si was evaporated from a solid thermal source using a pyrolytic graphite crucible. The Ge was evaporated from a solid thermal source by using a pyrolytic boron nitride crucible. The C beam was produced by sublimation from a graphite filament. Elemental boron was evaporated from a high temperature effusion cell with a graphite crucible inserted into a tungsten jacket.

Substrates were prepared by degreasing, etching and an HF dip. Growth occurred at substrate temperatures between 400 and 550 °C. The chemical composition has been deduced from linear extrapolations between the lattice constants in GeC and Ge by using X-ray rocking curve analysis, calibrated from higher C concentrations measured by resonant Rutherford backscattering spectroscopy (RBS). X-ray measurements were carried out with a double-crystal diffractometer by using CuKα radiation. Measurement of the lattice constants of our epilayer perpendicular to the surface a(were performed by a conventional Θ-2Θ scanning diffractometer with the symmetrical (004) reflection. Because C detection in random orientation with RBS yields the total of substitutional and non-substitutional C, the actual substitutional C was expected to be even lower than we calculated in Table 1. The chemical composition for a Ge-rich SiGeC alloy was measured by X-ray photoelectron spectroscopy (XPS) and secondary ion mass spectrometry (SIMS). Small values of the C concentration can be detected with resonant RBS using the resonance technique at 4.26 MeV.

We also found that SIMS is relatively insensitive to C when using O for sputtering. SIMS was applied to investigate the Boron distribution within our samples. Boron profiles are uniform throughout the layer for all our samples.

	Carbon (%)	Strain	E_g (eV) (FTIR)	E_g (eV) (response)	E_{ph} (meV)
SGC102	0	2.8×10^{-3}		0.66	14
SGC83	0	2.8×10^{-3}	0.65		16
SGC103	0	2.4×10^{-3}		0.64	17
SGC81	0.27	3.1×10^{-3}		0.74	11
SGC80	0.27	2.7×10^{-3}		0.73	11
SGC82	0.27	3.2×10^{-3}		0.72	12
SGC84	0.33	2.6×10^{-3}		0.74	11
SGC73	7% Si, 2% C	N/A	0.80		18

Table 1. Summary of SiGeC sample properties.

Effects of Carbon on hole mobility

Hall effect measurements were carried out by using a standard van der Pauw structure with In contacts under a magnetic field of 5.0 KG. The layers are electrically isolated from the substrate by using a reverse biased p-n junction. The carrier transport occurs primarily in the p-type epitaxial layer due to sufficiently low leakage current.

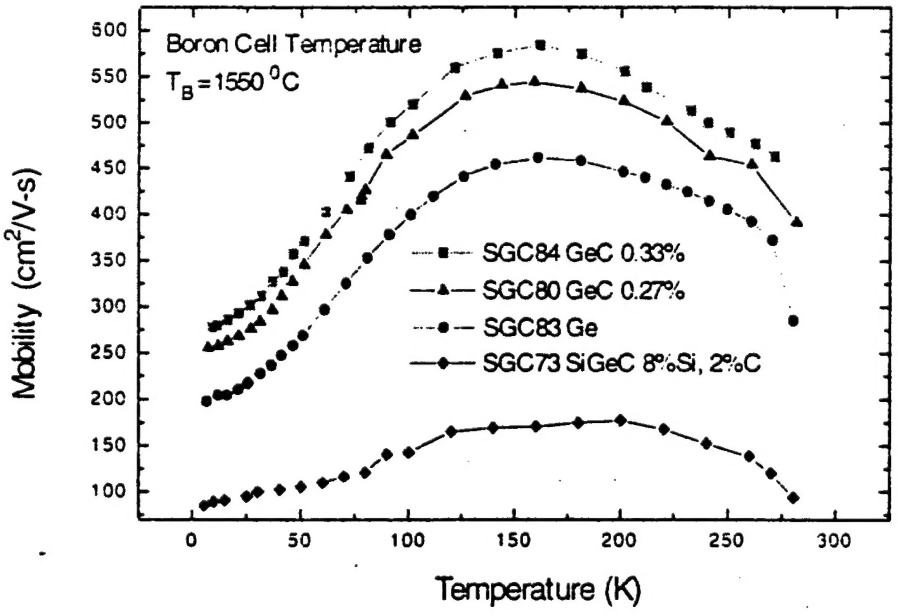

Figure 1 showing the hole concentration vs. Temperature measured by Hall effect measurements for four different alloy samples. At temperature range between 75K and 225K. their electrically active B concentrations were fairly close.

Figure 1 shows the characteristic temperature and hole concentration dependence of Hall mobility in four Ge-like crystal alloys. The mobility curves are constructed on the base of experimental data of Hall coefficient and resistivity, and we also assume a Hall scattering factor of unity. Sample SGC73 had slightly higher B concentration than other three samples. It indicates that the boron incorporation in SiGeC is slightly higher than in Ge and GeC. At room temperature, the B is almost 100% electrically active, and it points out that all dopants become incorporated into substitutional positions.

We plot the hole concentration dependence of Hall mobility in Fig. 2. It is still clearly seen that the sample with the highest C concentration has the highest mobility. From Fig. 2, we see that two GeC samples and one pure Ge sample have a similar doping level. We will concentrate our comparison mainly on these three samples. In Fig. 1 we found that the hole mobility increased with increasing C. The maximum mobility for all three sample occurs at temperatures near 150K.

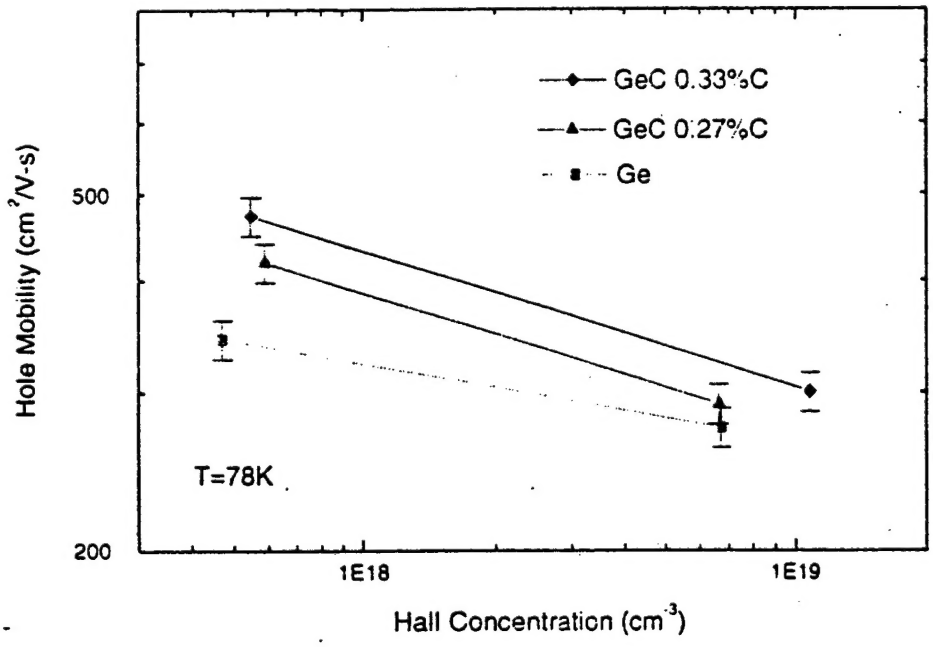

Figure 2. Hall effect measurements of the mobility of free holes versus the hole concentration. Solid line corresponds to the relation for pure Ge. The hole mobility of GeC alloy on Si substrate is a factor of three higher than in pure Si.

Additional carbon in the Ge will cause aperiodic potentials (if carbon atoms are introduced in substitutional positions) due to strong local lattice deformation near the C atoms, and high local strain fluctuation due to non-uniform C distribution, and extra neutral impurities (if carbon atoms become interstitial). These effects may increase the scattering rates, and thus reduce the carrier mobility. However, there are several possibilities for C to produce a net increase in mobility. One possibility is the carbon effect on grain boundaries and defects. Other possibilities are that carbon affects the effective mass of carriers, interface mismatch scattering, and intersubband scattering. The crystal quality could be determined by X-ray diffraction measurements. The average grain diameter D, which indicated the crystal quality was estimated from the full width at half maximum (FWHM) of the (004) X-ray diffraction line.

	Thickness (um)	Boron cell temperature (^{0}C)	X-ray FWHM (θ)	Mean surface roughness (nm)
Si_{1-y}-$Ge_{x-z}C_{0.02}$	0.18	1550	0.497	15.21
Ge	0.59	1550	0.310	0.473
$Ge_{0.9973}C_{0.0027}$	0.56	1550	0.290	0.347
Ge_{1-x}-$C_{0.0033}$	0.59	1550	0.139	0.308

Table II showing the surface roughness from AFM, and the full width at half maximum (FWHM) of the (004) X-ray diffraction line.

Adding more carbon in Ge can greatly improve the crystal quality, thus increasing the grain boundary size and decrease the amount of defects. This X-ray FWHM of (004) peak intensity result is consistent with our mobility analysis. How the carbon improves the crystal quality still needs further investigation. SGC73 (SiGeC) has the worst crystal quality, highest B doping concentration, and biggest compositional difference, thus the smallest mobility.

2. Current Voltage Characteristics of GeC/Si Heterojunction Diodes

The characteristics of heterojunction diodes fabricated from p-type epitaxial SiGeC alloy grown on an n-type (100) Si substrate were examined. The temperature dependence of the current-voltage behavior,

and measurements of the Hall effect, capacitance and optical absorption suggest that transport occurs by thermionic emission of electrons from the Si into the SiGeC, and that reverse breakdown occurs by the avalanche mechanism.

The major drawback in the use of SiGe/Si for high performance electronic devices is the relatively large lattice mismatch between Si and Ge (4%). Such a mismatch leads to the formation of strain-relieving misfit dislocations if the layer thickness exceeds a critical value. The dislocations may introduce states in the bandgap due to their strain fields and dangling bonds existing at their cores. As a result, they can introduce a large concentration of generation-recombination centers that will result in increased reverse leakage current and decreased breakdown voltage.

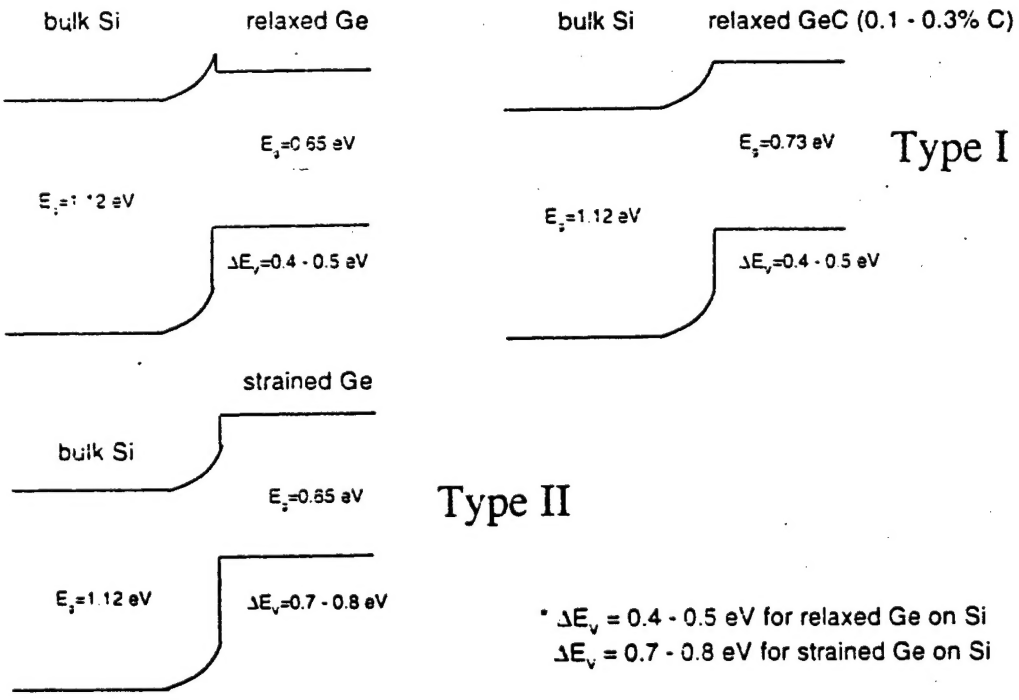

Figure 3. Schematic band diagrams showing energy offsets for heterojunctions of strained and unstrained Ge on Si, and our results for GeC alloys on Si.

It has been demonstrated that the addition of C during MBE can strongly affect the structural properties of GeC and SiGeC. Since all other processing parameters have been held constant, we expect that the

incorporation of carbon will significantly affect the I-V characteristics through the influence on structural properties. The possible effects of carbon on electrical properties are to reduce the mismatch between the hetero-interface, reduce the surface recombination velocity, change the bandgap and band offsets, and introduce localized strain that pins the propagation of dislocations.

Results and Discussions

Standard optical lithography and wet chemical etching were used to form the SiGeC/Si and GeC /Si HJ diodes. Ti/Au metal contacts of thickness 30 nm /150 nm were evaporated using an electron beam system. The standard lift-off method was used to form the completed structure. The Ti/Au contacts were measured to have Ohmic, linear current voltage characteristics over the full measurement range. The mesa area was 2.2×10^{-3} cm^{-2} for all our diodes.

The reverse-diode characteristics are summarized in Fig. 4, which shows the leakage current and reverse breakdown voltage. The leakage current appears to decrease and the reverse breakdown voltage appears to increase due to addition of C. Small amount of carbon (0.3%) in Ge can greatly reduce the reverse leakage current. Fig. 5 shows the forward I-V curves for several samples. It turns out that C can increase the turn-on voltage in the order of 0.1V by the amount of 0.3%C in Ge. The SiGeC/Si diode has the smallest reverse leakage current and the highest turn-on voltage, which are related to its highest carbon concentration and smallest lattice constant. Our I-V results indicate that the incorporation of C into SiGe and Ge produces better characteristics with smaller leakage current, higher breakdown voltage and higher turn-on voltage.

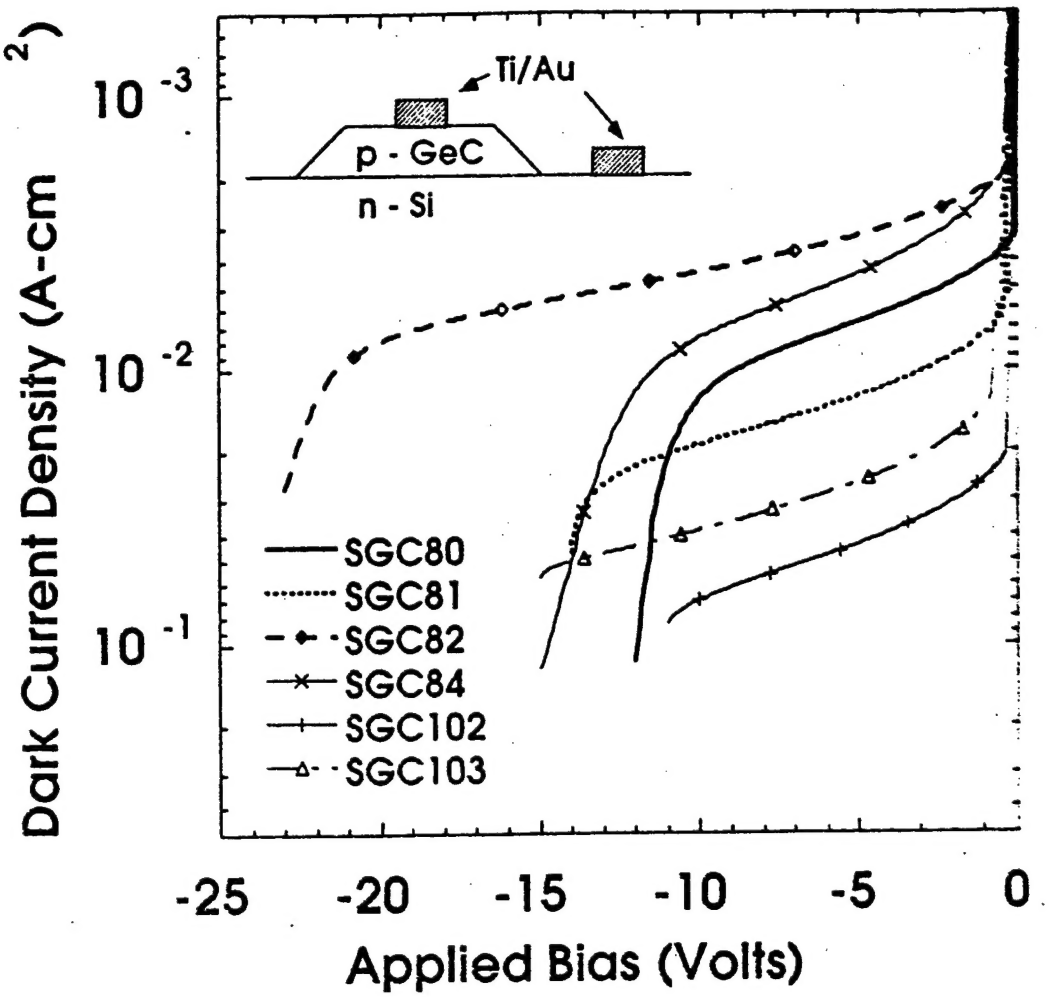

Figure 4. Reverse current density versus reverse bias voltage of p-N type $Ge_{1-y}C_y$/Si heterojunction diodes on Si (001) substrates with different composition, given in Table I. The reverse leakage currents decreased significantly with C fraction and with doping concentration. The inset shows the diode structure.

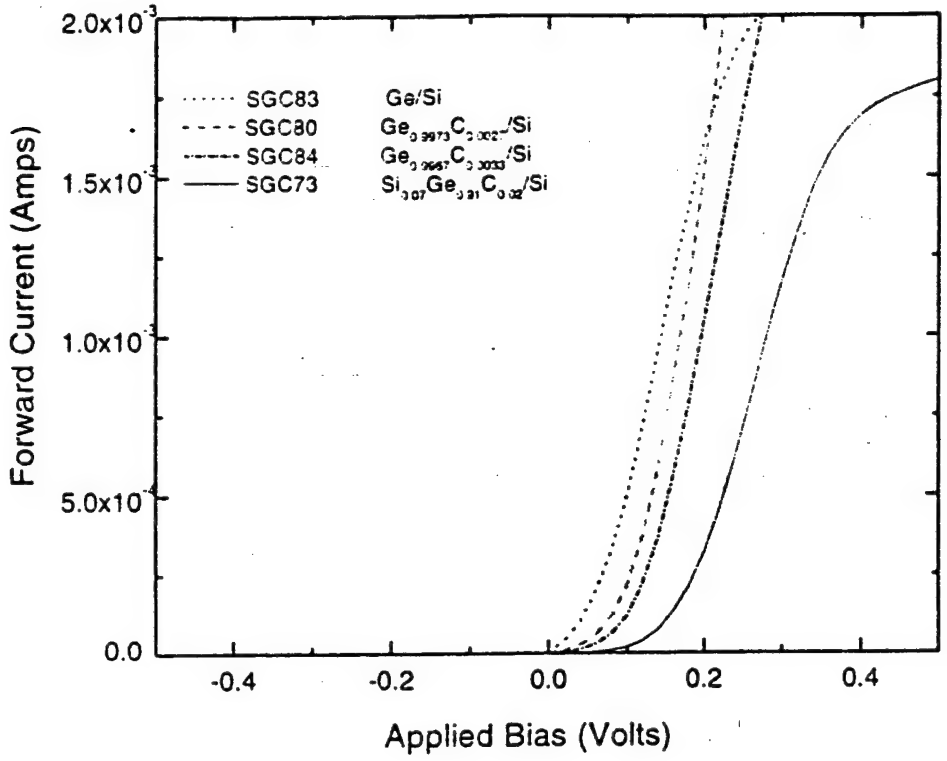

Figure 5. Forward I-V characteristics of mesa etched diodes fabricated in 0.2 micron thick p-SiGeC layer on n-Si(100) substrate. Current increases exponentially with temperature.

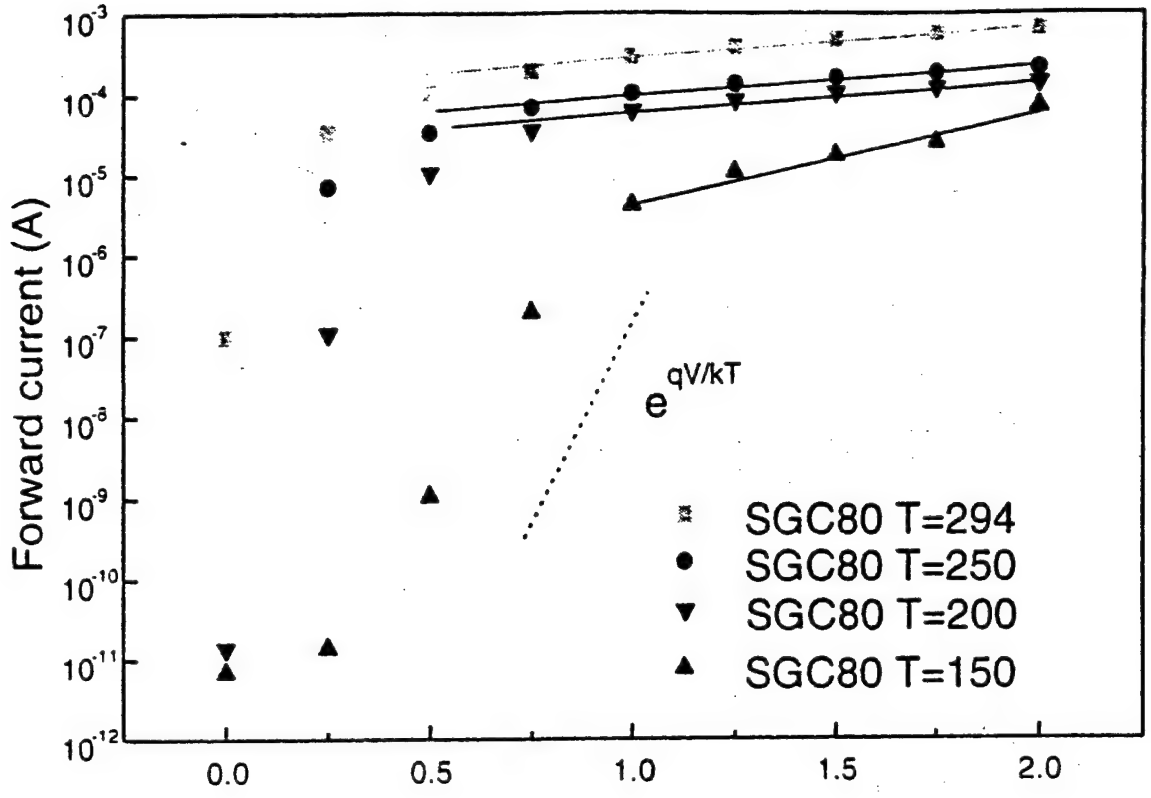

Figure 6. Temperature dependence of diode forward current. Behavior indicates a thermionic emission mechanism.

3. Size Distribution of SiGeC Quantum dots Grown on Si (311) and Si (001) surfaces

Quantum dots of $Si_{1-x-y}Ge_xC_y$ alloys with high Ge contents were grown on Si(311) and Si(001) substrates by solid source molecular beam epitaxy and were measured by atomic force microscopy. The quantum dot layers had a nominal thickness (equivalent two-dimensional) of 4 nm. The smallest quantum dots occurred for the composition $Si_{0.09}Ge_{0.9}C_{0.01}$ on Si (311), and had a 40 nm mean diameter, an 8nm mean height, and a density of $3.3x10^{10}cm^{-2}$. Quantum dots on Si(001) were larger and had less regular spacing than quantum dots on Si(311) with the same composition. Carbon decreased both the mean size and spacing of SiGe quantum dots and the ratio of size deviation to mean diameter. The presence of small uniform quantum dots for particular compositions is attributed to a reduction in the surface migration of adatoms due to decreased atomic surface diffusivity. These results suggest that

quantum dot organization is controlled by composition, substrate orientation, strain, and surface diffusion.

Introduction

Recent interest in low dimensional nanostructures is motivated by the possibility of new electrical and optical properties compared to bulk and 2-dimensional (2-D) layers. Sufficiently small structures are expected to exhibit quantum confinement effects at room temperature, short propagation delays, and Terabit-cm^{-2} densities[i]. Ge grows on Si by the Stranski-Krastanov mode of 2-D wetting for the first three monolayers, followed by three-dimensional (3-D) islanding. This islanding process can be utilized to achieve self-assembled quantum dot arrays. Such self-assembled or self-organized quantum dots on Si substrates are being investigated for producing nanostructures compatible with Si circuit processing. The fabrication of nanostructures by self-organization during epitaxial growth avoids the limitations of conventional lithographic processing. The question is whether the resulting quantum dot arrays will have the uniformity of sizes and positions suitable for device applications.

Quantum dot formation may be affected by substrate orientation through differences in surface energy, bond density and diffusivity. The growth of Ge quantum dots on Si has been investigated for the Si(001), Si(110), Si(111), and Si(311) orientations. It has been shown that Ge layers relax more readily on Si(001) than on Si(111) and maintain purely 2-D growth for slightly thicker layers on Si(311) than on Si(001). Additionally, the growth of SiGe quantum dots on Si (001) was found to depend on surface diffusion Quantum dot formation has been observed in the GeC system with optical properties depending on the C fractions. The formation of Ge islands on Si can be suppressed by using surfactants such as Ga and Sb and by reducing the substrate temperature to below 300°C. Adding C to SiGe alloys adds flexibility and has been studied in thin films[ii] but not previously in quantum dot layers. In this letter, we report on the size distribution of SiGeC quantum dots grown on Si(311) and Si(001) surfaces, and compare the effects of composition, strain, and substrate orientation.

Experiment

The samples were grown by solid source molecular beam epitaxy (MBE). Solid thermal sources were used for Si and Ge, and a heated graphite filament was used for C. The substrate temperature was 600°C for all layers. X-ray diffraction indicated that these conditions typically produce single-crystal epitaxial layers oriented with the substrate, for thick layers. The Si atomic fraction was varied from 0 to 0.1, and the C fraction was varied from 0 to 0.01. No surfactants, such as atomic H, were used during growth. The nominal thickness was 4nm, which is the thickness of an equivalent flat layer having the same volume as the quantum dot layer. The compositions were inferred from growth conditions calibrated by Rutherford Backscattering Spectrometry and by electron microprobe measurements of thicker samples grown under identical conditions.

The layers were examined by Atomic Force Microscopy (AFM), performed with a Digital Instruments Nanoscope III using the tapping mode technique with single crystal Si cantilevers having a nominal tip radius of 10nm. All samples were taken from the center of the wafer. To further ensure that the results were not due to local temperature variations several AFM scans were taken across the diameter of each wafer. The size and spacing data in Table III were obtained by analyzing the features from AFM scans. The quantum dot area was taken at a vertical position located 2 times the root mean square (RMS) surface roughness away from the mean baseline 2D surface. The quantum dot diameter is calculated from the quantum dot area assuming a circle of the same area as the quantum dot.

Result And Discussion

Fig 7a shows a top view of SiGe quantum dots on Si (311) together with the quantum dot-area distribution. Both large coalesced quantum dots and small coherent quantum dots are present in this sample. The size distribution shows a peak for large quantum dots at about 90nm diameter and a somewhat broader peak for small quantum dots at 35nm. Between these two maxima quantum dots of all sizes exist at a fairly constant rate. Quantum dots grown under similar conditions but containing C are shown in Fig. 7b. The presence of C decreased the mean size of the quantum dots, reduced the range of feature sizes as will be shown later by Fourier analysis, and narrowed the quantum dot size

distribution to only one strong peak at 40nm quantum dot diameter. SiGeC samples grown under identical conditions on Si (001) substrates showed that C had similar effects on the quantum dot size distribution and quantum dot feature sizes, however, the effect was less pronounced than for samples grown on (311). This indicates that the substrate orientation affects the quantum dot size. The addition of C to Ge quantum dots grown on (311) substrates yielded only a slight reduction in size and quantum dot spacing. We attribute the reduced effect of C on pure Ge to low substitutional incorporation of C in Ge. Statistics for all layers discussed above are given in Table III. As indicated in Table III, over the range of compositions and substrate orientations investigated, the smallest quantum dots were obtained for SiGeC compositions on Si(311). It is also significant that although smaller quantum dots are expected to have a smaller deviation of sizes, C reduced the ratio of quantum dot size deviation to quantum dot diameter, indicating higher regularity in SiGe layers containing C.

To determine the distribution of sizes, Fourier analysis was performed. The Fourier transform is proportional to the number of occurrences of the spatial wavevector, k. The spatial wavelength, $2\pi/k$, is the characteristic length associated with periodic spatial variations, including diameters, spacings, and vertical slopes of quantum dot edges. Two types of Fourier transforms were performed on the surfaces: 2-D based on the two-axis (x-y) raster scans, and one-dimensional (1-D) based on only the x-coordinate of sequential line scans. The 2-D spectrum showed circular symmetry, indicating no preferred orientation on any of the substrates. The 1-D Fourier intensity power spectrum, the square of the Fourier transform, is plotted versus spatial wavelength in Fig. 8, for the quantum dots of Fig. 7. The addition of C to SiGe reduced the mean value and the relative-range deviation of the quantum dot wavelengths. The Si(311) quantum dots had a smaller size and range than the Si(001) quantum dots; possible reasons for this include differences in the energies, bond densities, and atomic diffusion coefficients of the two surfaces. It is worth noting in Fig. 8 that the Fourier spectrum of sample SGC-180 had low intensities at wavelengths from 200nm to 800nm indicating significantly more uniformity than the other samples.

It is known that the addition of Si and C to Ge reduces the lattice mismatch to the Si substrate, thus increasing the critical thickness at which Stranski-Krastanov islanding occurs. The critical thickness t_c is proportional to the misfit ε with $t_c \propto \varepsilon^{-1}$. Adding 10% Si to Ge increases the critical thickness by

about 2ML. Substitutional C will also increase the critical thickness. We believe that a higher critical thickness results in an array of quantum dots with higher quantum dot density at the thickness immediately after the transition from 2D growth to 3D growth. This and reduced surface diffusion due to the incorporation of Si and C, which reduces the average bond length of the alloy and hence increases the diffusion barrier for surface adatoms could be responsible for the more evenly distributed smaller quantum dots observed in samples containing Si and C. The increased barrier against surface diffusion will decrease the coalescence of quantum dots into larger sizes, and thus a more closely spaced distribution of smaller quantum dots will be expected. The smaller and more regular quantum dot layers on Si (311) compared with Si(001) substrates may be due to surface-related differences including diffusivities, local strain, and critical thickness. For $Si_{0.1}Ge_{0.9}$ and $Ge_{0.99}C_{0.01}$ quantum dots under equivalent strain conditions, we found SiGe quantum dots to be smaller than GeC quantum dots, indicating that the chemical nature of the alloy affects quantum dot size in addition to strain.

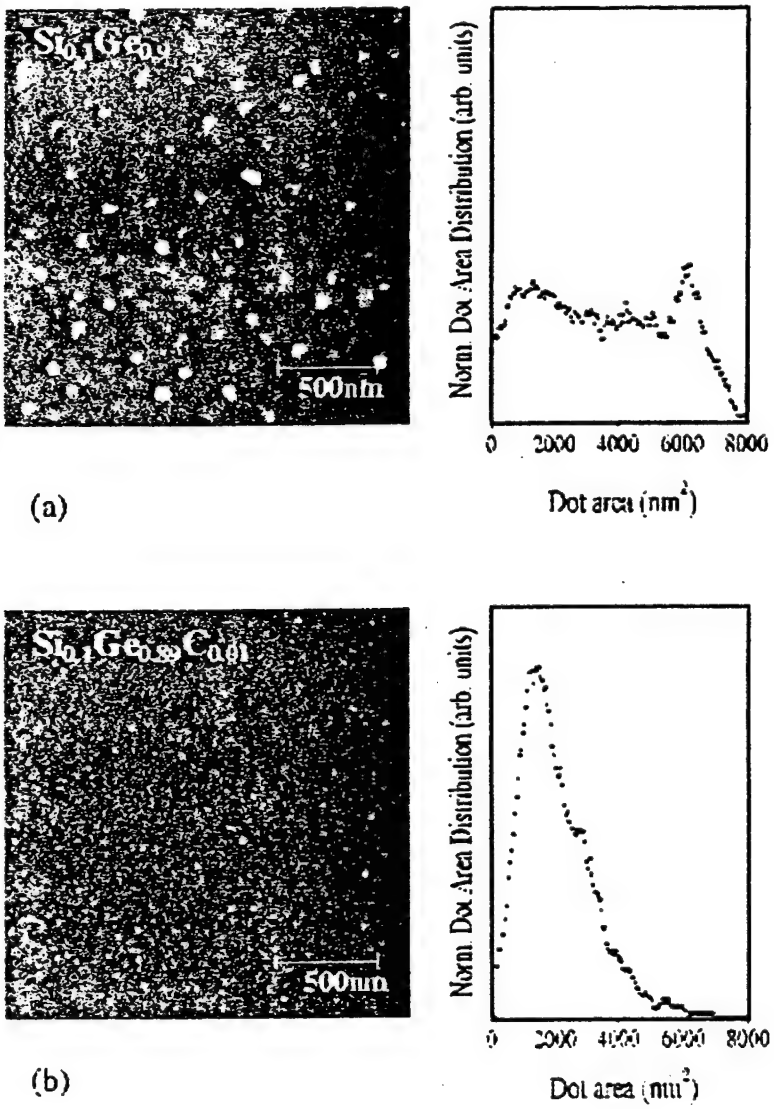

Figure 7 (a) Atomic Force microscopy scan of 2μm x 2μm area of $Si_{0.1}Ge_{0.89}$ grown on (311) Si and quantum dot area distribution (b) Atomic Force microscopy scan of 2μm x 2μm area of $Si_{0.1}Ge_{0.89}C_{0.01}$ grown on (311) Si and quantum dot area distribution. The curves were normalized by multiplying the number of equally sized quantum dots with their area and dividing the result by the scan area.

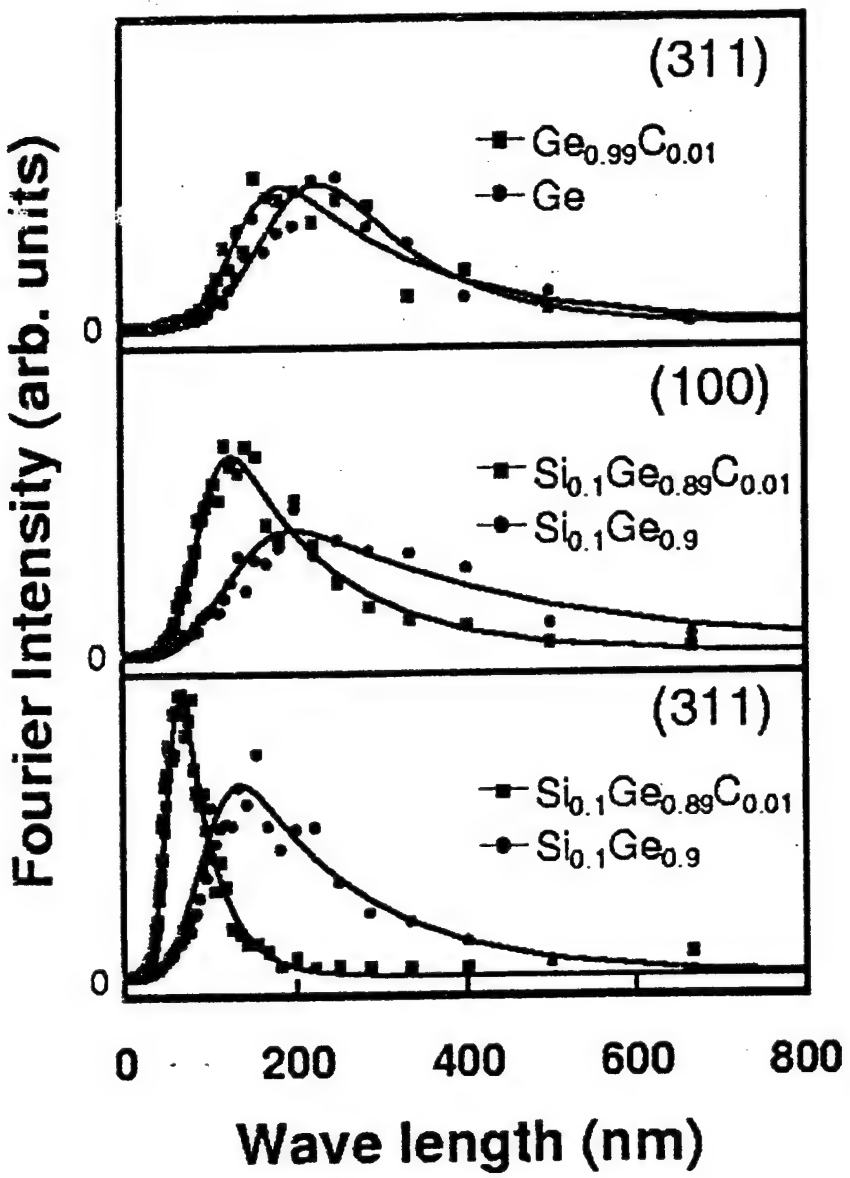

Figure 8. Fourier intensity distribution spectrum versus quantum dot partial wavelength for Ge, GeC, SiGe and SiGeC quantum dots on Si (311) and Si (001), obtained from AFM scans of Fig. 7., over the 2μm x 2μm area Markers represent measured data, solid lines were calculated by fitting the measured data to an exponentially altered Gaussian.

Table III. Nanostructure properties including composition, orientation of Si substrates, and statistical properties of quantum dots for 2 um X 2 um AFM scans of samples. Dev/Dia is the standard deviation of the diameter distribution divided by the diameter.

Sample No.	Composition	Subs. orien.	Dot Diameter [nm]	Peak Wavl. [nm]	Dot Density [cm^{-2}]	Av. Dot Height [nm]	Dev /Dia
SGC191	$Si_{0.1}Ge_{0.9}$	(311)	70	141	$7x10^{9}$	9.1	0.86
SGC180	$Si_{0.09}Ge_{0.9}C_{0.01}$	(311)	40	64	$3.4x10^{10}$	7.6	0.61
SGC183	$Si_{0.1}Ge_{0.9}$	(001)	71	207	$6.7x10^{9}$	12.8	1.23
SGC181	$Si_{0.09}Ge_{0.9}C_{0.01}$	(001)	58	125	$1.2x10^{10}$	11.5	0.98
SGC204	Ge	(311)	105	231	$2.5x10^{9}$	16.5	0.79
SGC205	$Ge_{0.99}C_{0.01}$	(311)	95	186	$3.0x10^{9}$	15.6	0.74

4. Conclusions

In this report, the electrical properties of SiGeC and GeC alloys have been examined. Effects of additional carbon on both carrier mobility and I-V characteristic have been demonstrated. Incorporation of carbon in Ge can increase the carrier mobility for thin GeC epilayers. Extra carbon in SiGe and Ge can decrease the average lattice constant, affect the interface states, influence the surface recombination velocity, change the bandgap and band offsets, and block the propagation of dislocations. These result in a better I-V characteristic with smaller leakage current and higher breakdown voltage. Our electrical study indicated that by careful control the growth conditions and carbon percentages, high-quality devices could be fabricated.

We have grown Ge, SiGe, GeC, and SiGeC quantum dots on (001) and (311) Si substrates. Quantum dots containing Si and C have smaller size and spacing for both (001) and (311) surfaces, and reduced deviations in size and spacing, which is crucial to applications requiring uniformity. The effect of C is stronger for alloys containing small amounts of Si, and is more prominent for alloys grown on (311) substrates. Differences between strain equivalent SiGe and GeC layers grown on (311) surfaces indicated that strain alone does not determine the geometry of quantum dot layers. These results indicate that strain, composition, and substrate orientation all play roles in quantum dot formation and provide different vehicles to control the self-assembly and self-organization of quantum dots for device applications.

SiGeC and GeC alloys may open up an exciting new region for heterojunction devices with Si technology compatible applications.

5. Bibliography

1. B. Orner, A. Khan, D. Hits. F. Chen, K. Roe, J. Pickett, X. Shao, R.G. Wilson, P. R. Berger and J. Kolodzey, ``Optical properties of GeC alloys," J. Electronic Materials, vol. 25, pp. 297-300, 1996.

2. F. Chen, B. Orner, S. Ismat Shah, M. M. Waite, S. S. Iyer and J. Kolodzey, ``Measurements of energy band offsets of SiGe/Si and GeC/Ge heterojunctions," Appl. Surface Science, vol. 104-105, pp. 615-620, 1996.

3. B. A. Orner, D. Hits, J. Kolodzey, F.J. Guarin, A.R. Powell, and S. S. Iyer, ``Optical absorption in alloys of Si, Ge, C, and Sn," J. Appl. Phys., v. 79, pp. 8656-8659, 1996.

4. B. A. Orner, J. Olowolafe, K. Roe, J. Kolodzey, T. Laursen, J. W. Mayer and J. Spear, "Bandgap of Ge-rich SiGeC alloys," Appl. Phys. Lett., vol. 69, pp. 2557-2559, 1996.

5. F. Chen, B. A. Orner, D. Guerin, A. Khan, P. R. Berger, S. Ismat Shah, and J. Kolodzey, ``Current transport characteristics of SiGeC/Si heterojunction diodes, " IEEE Electron Device Lett., v. 17, pp. 589-591, 1996.

6. J. Kolodzey, F. Chen, B. A. Orner, D. Hits, M. M. Waite, S. Ismat Shah, and K. M. Unruh, ``Energy band offsets of SiGeC heterostructures," Thin Solid Films, v. 302, pp. 201-203, 1997.

7. B. A. Orner, and J. Kolodzey, ``SiGeC alloy band structures by linear combination of atomic orbitals," J. Appl. Phys., v. 81, pp. 6773-6780, 1997.

8. F. Chen, R. T. Troeger, K. Roe, M. D. Dashiell, R. Jonczyk, D.S. Holmes, R.G. Wilson and J. Kolodzey, ``Electrical properties of SiGeC and GeC alloys," *J. Electronic Materials*., v. 26, pp. 1371-1375, 1997.

9. B. A. Orner, F. Chen, D. Hits, M. W. Dashiell, and J. Kolodzey, ``Optical constants of B and P doped GeC alloys on Si substrates," in *SPIE Optoelectronics:* '97: *Silicon-Based Monolithic and Hybrid Optoelectronic Devices*, Proc. SPIE Proc. vol. 3007, pp. 152-161, 1997.

10. M. W. Dashiell, R. T. Troeger, L. V. Kulik, A-S. Khan, F. Chen, K. Roe, B. A. Orner, P. R. Berger, J. Kolodzey, and R. G. Wilson, ``Electrical and Optical Properties of Phosphorus Doped GeC{0.001}," Seventh International Symposium on Silicon Molecular Beam Epitaxy in Banff, Canada}, (July 13-17, 1997), Thin Solid Films, v. 321, pp. 47-50, 1998.

11. M.W. Dashiell, L.V. Kulik, D. Hits, J. Kolodzey, and G. Watson, ``Carbon incorporation in SiC alloys grown by molecular beam epitaxy using a single silicon-graphite source," Appl. Phys. Lett., v. 72, pp. 833-835, 1998.

12. L.V. Kulik, D. Hits, M.W. Dashiell, and J. Kolodzey, ``The effect of composition on the thermal stability of SiGeC/Si heterostructures," Appl. Phys. Lett., v. 72, pp. 1972-1974, 1998.

13. R. Jonczyk, D. A. Hits, L.V. Kulik, J. Kolodzey, M. Kaba, and M. Barteau, ``Size distribution of SiGeC dots grown on Si(311) and Si(100) surfaces," J. Vac. Sci. Tech., v. B 16, pp. 1142-1144, 1998.

14. J. Kolodzey, O. Gauthier-Lafaye, S. Sauvage, J.-L. Perrossier, P. Boucaud, F.H. Julien, J.-M. Lourtioz, F. Chen, B. A. Orner, K. Roe, C. Guedj, R.G. Wilson, and J. Spear, "The Effects of Composition and Doping on the Response of GeC/Si Photodiodes, " IEEE Journal of Selected Topics in Quantum Electronics, v. 4, pp. 964-969, Nov./Dec. 1998.